

Monte Carlo study of liquid-crystal ordering in the independent-pore model of aerogels

T. Bellini,^{1,4} C. Chiccoli,² P. Pasini,^{2,4} and C. Zannoni^{3,4}

¹*Dipartimento di Elettronica, Università di Pavia, via Ferrata 1, 27100 Pavia, Italy*

²*Istituto Nazionale di Fisica Nucleare, Sezione di Bologna, Via Irnerio 46, 40126 Bologna, Italy*

³*Dipartimento di Chimica Fisica ed Inorganica, Università di Bologna, Viale Risorgimento 4, 40136 Bologna, Italy*

⁴*Istituto Nazionale per la Fisica della Materia, Italy*

(Received 26 January 1996)

We have performed Monte Carlo simulations of a confined Lebwohl-Lasher nematic model with different boundary conditions to verify the appropriateness of the independent pore approximation for liquid crystals in silica aerogel systems. We find evidence for the need of going beyond independent pores to account for calorimetric and turbidity data at the same time. [S1063-651X(96)09808-X]

PACS number(s): 61.30.Cz, 61.30.Gd, 64.70.Md

I. INTRODUCTION

The phase behavior of fluid systems confined in porous hosts is a topic of wide current interest in condensed matter physics, probably because it stands at the crossroads of several issues of general importance, such as the effects of finite size and quenched disorder. The isotropic to nematic phase transformation of thermotropic liquid crystals embedded in a number of porous matrices has been experimentally characterized using various techniques [1]. In particular, a large effort has been devoted to study the thermodynamic, optical, and dynamic properties of liquid crystals incorporated in low density silica aerogels [1]. Silica aerogels have a solid phase density which may be as low as a few percent in volume fraction and their microscopic structure is a networklike skeleton of multiply connected silica strands [2]. Such twigs have surface roughness and mean diameter typically of about 40–70 Å [2]. It has been found that silica aerogels have a disordering effect on the nematic and smectic phases of liquid crystals, probably resulting from the combined effect of the random orientation of the silica strands and of the strong surface coupling between silica and liquid-crystal molecules. Analogous reductions in the nematic order parameter have been found by studying liquid-crystal alignment near random surfaces obtained by silica evaporation [3]. It is generally known that bare flat silica surfaces strongly induce planar alignment, while lecithin treated silica surfaces show weak homeotropic coupling [4]. The large reduction of the disordering effect of the aerogel observed after lecithin treatment [5] is a further proof that the silica strands strongly favor random but well determined positions and orientations of the liquid-crystal molecules on their surface. The low density and the fine structure of the silica aerogels make them the best experimental realization of the random field disturbances, widely studied theoretically [6]. A mean field solution to the Lebwohl-Lasher model [7] with added random field has recently been proposed to understand the observed behavior of the isotropic to nematic transition in silica aerogel [8].

Experimentally, it has been found that the disturbances induced by the silica aerogel effectively modify the properties of the liquid crystals. Long range order is suppressed, thermodynamic singularities become rounded, and local

nematic and smectic ordering is achieved via a generally smooth growth spread out in large temperature intervals. The basic experimental observations can be understood by modeling the silica aerogel as a true porous material, having independent pores and characterized by a given pore size distribution [9–11]. Of particular interest here are the calorimetry measurements, which show a progressive depression of the transition temperature and a gradual rounding of the specific heat peaks when the density of the aerogel is increased [12]. A phenomenological scaling behavior of the transition temperature shifts and of the transition enthalpy as a function of pore size can be obtained by associating to each aerogel its mean pore size. Since such a scaling behavior cannot be interpreted as a pure finite size effect on the phase transitions [10], an analysis of the effects on the specific heat due to the specific coupling between liquid crystal and pore surface would be of particular interest.

The mean size of the cavities within an aerogel and their statistical distribution can in turn be extracted from an appropriate analysis of the empty aerogel structure factor as measured by small angle x-ray scattering [9]. Since the calorimetric quantities, relevant for the comparison between simulation and experiment, can be thought of as a superposition of contributions from the different pores having different sizes, and since the enthalpy exchanged from each pore is roughly proportional to its volume, the best estimate of the mean pore size of each aerogel is obtained by weighting each pore with its volume. The pore sizes of the silica aerogels obtained by this volume averaging procedure range from 240 Å to 1400 Å [9].

The aim of the present paper is to explore the independent-pore approximation in better detail. Its success in interpreting most of the experimental results relies, in fact, on quite approximate arguments, e.g., in assuming that the nematic or smectic order parameter is constant within each pore [9]. On the other hand, some experimental evidences seem to indicate that such an approximation is not always appropriate. For example, the fact that the smectic correlation length is larger than the pore size for the lowest density aerogel [10], or the dynamic slowing down observed at the lowest temperatures of the nematic phase [9], suggests that the pore connectivity could play a significant role. Some simulations of the liquid-crystal ordering in silica aerogel

have already been proposed [8,13,14]. The comparison with the experimental results, however, is never discussed in any quantitative detail. When such a comparison is performed, the depression in temperature found by the simulation is about 25 times larger than in the experiment [13], as discussed more in detail below. In the present paper we study the nematic ordering within pores of different sizes having various boundary conditions and we compare the results with experiment in three ways: by comparing the transition temperature shifts and the transition enthalpy as obtained by calorimetric measurements [12], and by comparing the temperature dependence of the mean nematic order parameter as obtained by the optical turbidity measurements [9].

II. THE MODEL SYSTEM

Our model is based on the Lebwohl and Lasher (LL) [7] lattice spin model which has been extensively used in computer simulations of liquid crystals [15–17]. It consists of a system \mathcal{S} of “spins,” each represented by a headless unit vector \mathbf{u}_i , placed at the sites of a cubic lattice and interacting with a second rank pair potential

$$U = - \sum_{i,j \in \mathcal{S}} \epsilon_{ij} \left[\frac{3}{2} (\mathbf{u}_i \cdot \mathbf{u}_j)^2 - \frac{1}{2} \right] - J_B \sum_{i \in \mathcal{S}, j \in \mathcal{G}} \epsilon_{ij} \left[\frac{3}{2} (\mathbf{u}_i \cdot \mathbf{u}_j)^2 - \frac{1}{2} \right], \quad (1)$$

where ϵ_{ij} is a positive constant when the spins i and j are nearest neighbors and zero otherwise. The second part of the Hamiltonian serves to keep into account the interaction of the liquid crystal with the external environment \mathcal{G} . This is modeled by an additional layer of spins which have orientations fixed according to the direction imposed by the chosen boundary conditions B and coupling strength with the spins inside to the droplet defined by the parameter J_B . Here we have studied various types of boundary condition keeping fixed the value of anchoring $J_B = 1$. We recall that the LL model unlike the discrete orientation models reproduces the characteristics of a weakly first order nematic-isotropic phase transition as observed in real nematics [16,17] even though the molecules are fixed on the lattice sites. In particular the long range orientational behavior does not differ in any essential way from that of real nematics, as also indicated by the correct prediction of a correlation length divergence at a temperature slightly below the nematic-isotropic transition. The correct handling of orientational order and correlations seems particularly relevant for aerogels, where profound changes in behavior compared with the bulk are connected with the correlation length decaying on a scale similar to the pore size.

This model [18] has also proved to be useful in simulating nematic confined systems such as polymer dispersed liquid crystals (PDLC) [19] under various conditions of surface alignment (homeotropic and planar), anchoring at the droplet surface and external fields. Moreover we have shown that it is possible to reproduce from Monte Carlo (MC) simulations not only the thermodynamics, but also qualitatively correct experimental observables like deuterium NMR spectra and polarized microscopy textures [21,20].

In this work we investigate an approximately spherical nematic sample carved from a cubic lattice with spins interacting with the LL potential Eq. (1) [18]. We wish to examine which kind of boundary conditions best represents the effect of the silica network within the independent-pore approximation and thus we have studied toroidal, bipolar, three-dimensional (3D) random, and 2D random (tangential) orientation at the surface. Some of the results for these boundary conditions are available from our previous work [18,20,21]. Here we present results for a layer of outside “ghost” spins with fixed isotropic random orientations in three and two dimensions (3DI and 2DI). This provides a fixed random field acting only on surface particles, different from the random field acting on all particles as employed by Zhang [14] and found unsatisfactory for quantitative comparison with experiment. In addition to these different random boundaries, we have also studied a rather large system with bipolar boundary conditions as a model for weak ordering effects on the trapped nematic.

The present model is different in a number of ways from that employed in computer simulations by Uzelac *et al.* [13]. In that case a discrete orientation Potts model was used and a noninteracting silica network was built, using a diffusion-limited cluster-cluster aggregation method, inside the sample. However, the Potts model does not provide a satisfactory model for the bulk behavior of liquid crystals and moreover at a liquid-crystal concentration of 70% the shift in transition temperature from the bulk is predicted to be $\approx 25\%$ of its value that for 4-*n*-octyl-4'-cyanobiphenil (8CB) would correspond to more than 100 K compared to the observed value of ≈ 3 K.

All the simulations have been performed with a standard Metropolis procedure as described in detail in our previous papers [16,18]. Several thermodynamic observables have been calculated: energy U , dimensionless heat capacity C_V^* , overall second and fourth rank order parameters, $\langle P_2 \rangle_\lambda$ and $\langle P_4 \rangle_\lambda$, obtained from eigenvalues of the ordering matrix [15], and orientational correlation functions.

III. SIMULATION RESULTS

A. 3D random boundary conditions

We have performed a large number of simulations for system sizes ranging from 136 to 5832 spins each studied over a wide range of temperatures (about 40) and with 3D random boundary conditions. In practice the orientations of the spins in the external layer \mathcal{G} [cf. Eq. (1)] are assumed to be random in space and with a coupling to the nematic molecules $J_B = 1$. We find that the molecular organization inside the droplet appears to be dominated by the effects of the intermolecular potential which tends to align the spins parallel to each other. This can be quantitatively determined by dividing the droplet into concentric regions, as described in Ref. [18], and calculating the order parameter in each shell going from the center of the droplet toward the surface. The results in Fig. 1 clearly indicate a very small decay of $\langle P_2 \rangle_\lambda$ below the nematic-isotropic transition. At low temperature the molecules inside the droplet form an ordered domain, growing from the center of the sphere, that propagates up to the one or two layers nearest to the surface. Increasing the temperature the order, especially close to the surface, decreases and, above the N - I transition, only a small ordered core survives. The molecular interactions thus over-

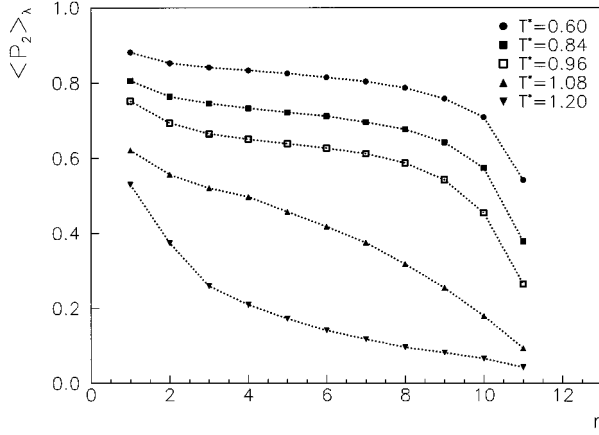


FIG. 1. The second rank order parameter, $\langle P_2 \rangle_\lambda$, for a droplet with $N=5832$ and 3DI boundary conditions, plotted against distance from the droplet center in lattice units, r , at various scaled temperatures $T^*=kT/\epsilon$.

come the disordering effect of the random boundary conditions which prove to be less influential in comparison with other kinds of surface alignment such as planar or homeotropic [20].

The standard orientational order parameter $\langle P_2 \rangle_\lambda$ calculated over the whole sample shows that the system goes smoothly from a quite ordered phase to an isotropic one (see Fig. 2). As mentioned above, the random boundary conditions lower the order near the surface and the overall $\langle P_2 \rangle_\lambda$ is reduced by approximately 20% in comparison with the value for the bulk at the same scaled temperature (circles in Fig. 2), obtained by dividing the temperature by that of transition for the bulk.

The orientational pseudotransition occurs in turn at a temperature lower than that of the bulk system that is approached from below as the size increases and is less sharp.

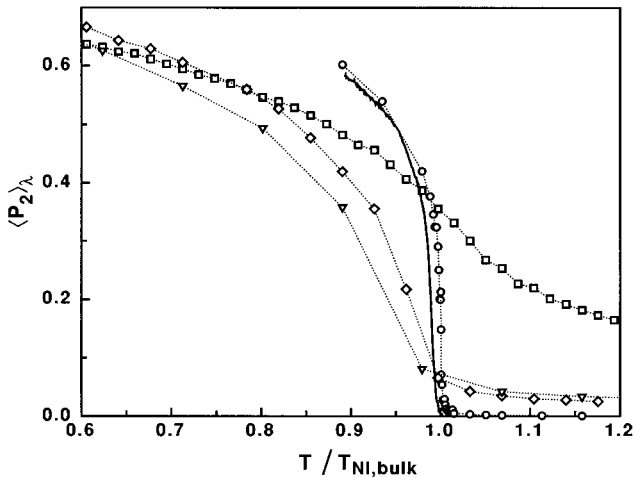


FIG. 2. The second rank order parameter, $\langle P_2 \rangle_\lambda$, for a droplet of 1472 particles with bipolar boundary conditions (squares) and 5832 particles with 3DI boundary conditions (diamonds) as a function of reduced temperature (temperature divided by the bulk NI transition temperature). We also show reference results for the bulk [16] (circles), a cylindrical sample with 3200 spins (triangles), and experiment [9] (continuous line).

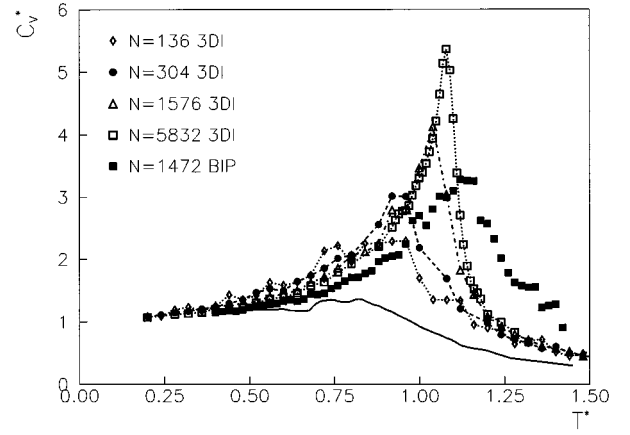


FIG. 3. Heat capacity, C_V^* of droplets with 3DI boundary conditions and different numbers of particles N versus scaled temperature T^* as obtained from the simulations. Results for a 1472 system with bipolar boundary conditions (BIP) are also reported. The continuous line represents the curve used as background (see text).

To test the effects of the sample shape on the results we have also performed a simulation of a cylinder containing 3200 spins with 3D random boundary conditions. The results seem to be unaffected by the sample shape and in particular the curves of the nematic order parameter, $\langle P_2 \rangle_\lambda$, versus temperature are rather similar.

The depression of the orientational phase transition is more apparent looking at the heat capacity, obtained by differentiating the energy as described in [22] and reported in Fig. 3. The peaks of the heat capacity decrease and are shifted to lower temperatures T_c as the system size decreases. In Table I we summarize the results for the systems studied.

B. 2D random

Trying to separate the effects of boundary conditions from that of the independent-pore assumption, we have also con-

TABLE I. A summary of the systems studied with the different boundary conditions (BC) employed. N_{part} are the molecules (spins) inside the sample while N_{ghost} are the particles at the surface (see text). The pseudotransition temperature, $T_c^* \equiv kT/\epsilon$, defined as the temperature corresponding to the C_V peak, and the maximum of the heat capacity $(C_V)_{max}$ are also reported.

BC	N_{part}	N_{ghost}	T_c^*	$(C_V)_{max}$	Ref.
3D Random	136	120	0.96 ± 0.02	2.9 ± 0.2	This work
3D Random	304	200	0.98 ± 0.02	4.3 ± 0.3	This work
3D Random	1472	552	1.06 ± 0.01	4.1 ± 0.2	This work
3D Random	5832	1352	1.08 ± 0.01	5.3 ± 0.1	This work
2D Random	304	200	0.94 ± 0.02	2.8 ± 0.2	This work
Radial	304	200	0.99 ± 0.02	2.0 ± 0.1	[18]
Radial	1568	576	1.10 ± 0.01	2.7 ± 0.2	[18]
Radial	5832	1632	1.10 ± 0.01	3.5 ± 0.1	[18]
Toroidal	304	200	1.06 ± 0.01	2.1 ± 0.1	[18]
Toroidal	1568	576	1.08 ± 0.02	2.8 ± 0.2	[18]
Bipolar	304	200	1.11 ± 0.01	2.6 ± 0.2	[21]
Bipolar	1472	552	1.12 ± 0.01	3.3 ± 0.1	This work

sidered the possibility that silica twigs are not random in 3D but rather that they can have a random orientation tangential to the sphere. Keeping the coupling J_B the same, we have performed simulations on a sample with $N=304$. We find, as shown in Table I, that the shift in T_c^* is of the same order of magnitude of that of the 3DI case for simulation of the same size sample.

C. Bipolar

Another possibility we have considered is that the silica twigs have, for instance because of relatively large connectivity (long twigs), an ordering effect. Such a possibility has been roughly modeled employing bipolar boundary conditions for which boundary layer molecules are directed along the meridians of the model droplet while being tangential to the surface. Here we have simulated a 1472 particle system while results for the smaller droplet are taken from Ref. [20]. The nematic ordering inside the sample, shown in Fig. 2 (squares), is favored by this kind of planar anchoring and, especially above the pseudotransition temperature, a more ordered system, in comparison with the other boundary conditions, remains. Consequently the shift in T_c^* is smaller, as can be seen from Table I, also for the smaller system considered. The variation of order inside the droplet has been reported elsewhere, albeit for a small system [21(c)].

IV. COMPARISON WITH EXPERIMENTS

The comparison between the experimental results obtained for the isotropic to nematic phase transition of 8CB in silica aerogel and the Monte Carlo simulation of the LL system in random pores can be performed by examining (i) the pore size dependence of the transition enthalpy obtained by integrating the C_V^* curve and normalized with respect to the bulk transition enthalpy; (ii) the pore size dependence of the shift of the transition temperature normalized with respect to the bulk; and (iii) the rescaled temperature dependence of the measured turbidity and the simulated order parameter.

In order to estimate the transition enthalpy ΔH , we notice first that for a real nematic the transition volume is very low [typically $(\Delta V_{NI}/V) \approx 0.4\%$] so that $\Delta H \approx \Delta U$ can be obtained from the lattice model simulations. Then, we have integrated the simulated C_V^* curve subtracting as background a smooth C_V^* curve. Experimentally the ‘‘singular’’ part of the measured specific heat is obtained subtracting a background with the appropriate low and high T values [12]. In the simulations we have generated a system exhibiting the correct limiting values of C_V and no transition temperature by dispersing a 20% fraction of random frozen spins in the lattice [23]. The obtained C_V curve, which we have used as a background, is shown in Fig. 3. In Fig. 4 we show $\Delta H/\Delta H_{bulk}$ for both the experiment and the simulation. The results from the simulations are plotted as a function of the inverse droplet size L (bottom axis), while the experimental results are plotted as a function of the silica volume fraction in the silica aerogels Φ_s (top axis). The independent variables have been chosen in this way because, according to the analysis of the aerogel structure, the aerogel density is with good approximation proportional to the inverse mean pore size [12]. The scale of the top axis of Fig. 4 has been selected

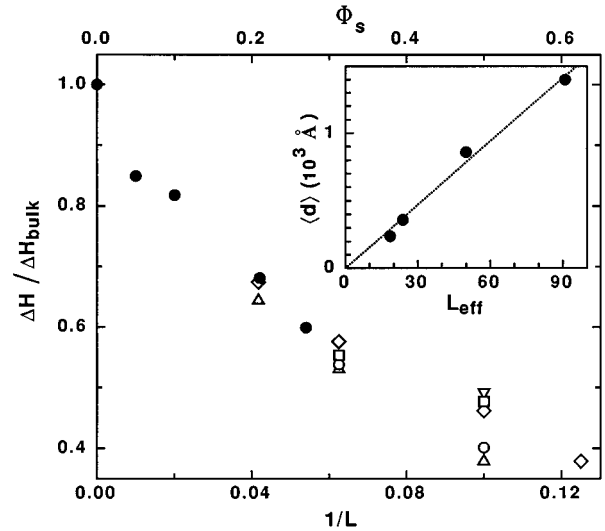


FIG. 4. Transition enthalpy, $\Delta H/\Delta H_{bulk}$, scaled by the bulk value for 8CB in a silica aerogel (full circles) [9] and simulations with radial (triangles up), 2DI (triangles down), 3DI (diamonds), bipolar (squares), and toroidal (circles) boundary conditions plotted against inverse diameter L (in lattice units) and the silica volume fraction in the silica aerogels Φ_s (top axis). The inset shows the relation between the real and lattice linear dimension (see text).

to produce the best overlap between experimental and simulated results and the result is actually a good match. In order to quantify the scale factor connecting top and bottom x axes of Fig. 4, we show in the inset a comparison between the volume-averaged pore size of the four densities of silica aerogels with the diameter $\langle d \rangle$ of the equivalent droplets as extracted by the bottom axis. The slope of the fitting line is $17 \pm 3 \text{ \AA}$, where the uncertainty gives an estimate of the range of the scale factor giving an ‘‘acceptable’’ overlap between experiment and simulation in Fig. 4 and accounts for the difference in the thermodynamic behavior induced by the different boundary conditions. From this analysis we conclude that the unit lattice distance in the simulation corresponds to a physical length of $17 \pm 3 \text{ \AA}$. Since the volume of the molecules used in the experiment (8CB) is approximately 480 \AA^3 [24] it follows that, in the simulation, each spin corresponds to a group of the order of ten molecules. This equivalent length, even though somehow smaller than the one previously obtained in other Lebwohl-Lasher simulations [20], confirms the hypothesis that each spin could represent a closely packed group of molecules that maintains its short range order across the nematic-isotropic phase transition [25]. It is worth noting that the boundary conditions have only a mild effect on $\Delta H/H_{bulk}$: by appropriately rescaling the droplet size by at most 20%, all the simulation results in Fig. 4 fall on the same curve.

We now turn to the ‘‘pseudotransition temperature.’’ We have extracted from the simulation results the ratio $T_c/T_{NI,bulk}$. With a choice of axes analogous to Fig. 4, Fig. 5 shows $T_c/T_{NI,bulk}$ for both experiment and simulation as a function of inverse droplet size and the silica volume fraction. Unlike what was found for $\Delta H/H_{bulk}$, it appears that the effect of the boundary conditions on the depression of the isotropic to nematic transition temperature is rather dramatic. The random boundary conditions induce a shift of the transition temperature which is about six times larger than the

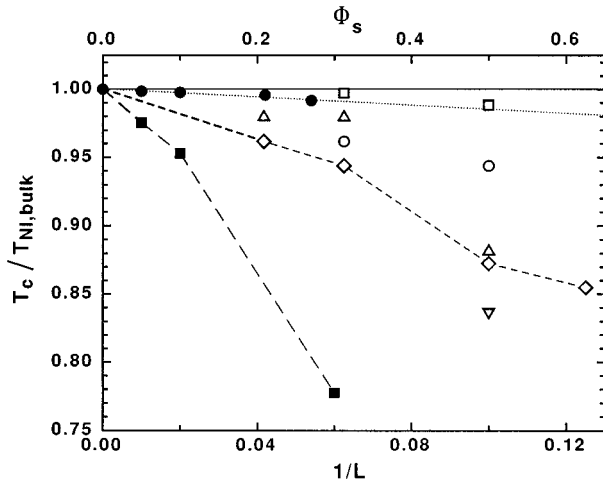


FIG. 5. The pseudotransition over bulk transition temperature for 8CB together with simulation results from this work (same symbols as Fig. 4) and from Uzelac *et al.* [13] (full squares).

one measured in the experiments on liquid crystal in silica aerogel. As shown in Fig. 5, in order to obtain a closer resemblance to the experimental results, more ordering boundary conditions could be used, such as the bipolar or the toroidal boundary conditions, although such a choice is harder to justify in terms of the aerogel structure. In Fig. 5 we also show the results by Uzelac *et al.* [13], as a function of the volume fraction of lattice sites filled by the perturbing gel-like branches (top axis). As is clearly evident, the temperature shift in Ref. [13] is much larger than the one obtained in our simulation scheme. The problem of obtaining a temperature shift comparable with the experimental ones is thus still an unsolved problem of the computer simulations so far presented of the liquid-crystal ordering in disordered geometries.

One of the most striking features of the liquid crystals in silica aerogel is that they are transparent in the isotropic phase and very turbid in the nematic phase, much more than their corresponding nematic bulk samples. By modeling the nematic phase within the aerogel as an ensemble of independent uniaxial domains having random optical axes, it has been shown that the measured optical turbidity can be expressed as a function of mean pore size, probing wavelength and birefringence within each pore [9]. The calculation was originally performed by assuming the birefringence to be constant within each nematic domain. Nevertheless, since the system is well inside the Debye-Rayleigh-Gans regime, and since the domain size is smaller than the optical wavelength [9], the birefringence within each domain contributes to the optical turbidity τ through its mean value over the domain. Since, in turn, the birefringence of a liquid crystal is with good approximation proportional to the nematic order parameter, the measured turbidity τ is a function of the average order parameter within each pore. Explicitly [9] $\tau = K \langle P_2 \rangle_\lambda^2$, where the constant K contains only temperature independent quantities. In Fig. 2 we show $\langle P_2 \rangle_\lambda$ as extracted by the experimentally measured optical turbidity in the sample, prepared by using the 0.36 g/cm^3 silica aerogel. The constant K used to produce the plot ($K = 120 \text{ mm}^{-1}$) is obtained by assuming the mean domain size in agreement

with the mean pore size of the aerogel in use [9]. As we can see, for $T < 35^\circ \text{C}$ the curve matches the bulk $\langle P_2 \rangle_\lambda$, indicating that the growth of the order parameter in the domains is similar to the one in the bulk, while for $T > 35^\circ \text{C}$ the difference between the two curves seems to be due to the combined effect of finite size and boundary conditions. By inspecting the curves obtained from the simulation, it appears that, while the random boundary conditions produce the correct temperature dependence of $\langle P_2 \rangle_\lambda$, namely, $\langle P_2 \rangle_\lambda = 0$ for $T > T_{NI,bulk}$ and a continuous dependence on T for $T < T_{NI,bulk}$, they also predict, as previously observed, too large a temperature shift. On the other hand, bipolar boundary conditions provide a much better estimate of T_c but produce a $\langle P_2 \rangle_\lambda$ with large nonzero values for $T > T_{NI,bulk}$, a consequence of the ordering effect of the boundary conditions. The most realistic $\langle P_2 \rangle_\lambda$ curve could probably be obtained from very large droplets having random boundary conditions.

V. CONCLUSIONS

We have performed Monte Carlo simulations of droplets with various types of boundary conditions in order to check if the independent-pore model of liquid crystals in silica aerogel systems is appropriate or not. Our results indicate that the most straightforward simplification of the silica aerogel structure, i.e., independent pores inducing 3D random boundary conditions, reproduces qualitatively the features observed in real experiments. However, from a quantitative standpoint it yields unsatisfactory predictions since it cannot reproduce at the same time both shift in temperature and depression in transition enthalpy. This fact suggests that the liquid-crystal ordering inside the silica gel network is strongly affected by the connectivity of the pores. Alternatively, such a quantitative discrepancy may also indicate that the coupling of the liquid-crystal molecules with the silica branches involves some more complicated surface phenomena not correctly modeled by assuming a complete randomness of the silica surface. In order to test this possibility, we have extended the comparison between experiment and simulation to different boundary conditions, some of them explicitly developed for this purpose. We find that if we want to maintain the independent-pore approximation a two sided problem exists. On one hand, boundary conditions having larger ordering effects than the random boundary conditions should be used in order to mimic the silica induced alignment. Bipolar and toroidal boundary conditions have indeed a calorimetric behavior which depends on the droplet size in a way similar to that observed in real experiments. On the other hand, the use of these ordering boundaries, at least the ones employed here, causes unsatisfactory temperature dependence of the order parameter and thus of the turbidity.

Thus we envisage the need of going beyond the independent-pore approximation to obtain a satisfactory representation of the liquid-crystal aerogel system in all its properties.

ACKNOWLEDGMENTS

We acknowledge support from MURST and CNR and useful conversations with N.A. Clark.

- [1] *Liquid Crystals in Complex Geometries Formed by Polymer and Porous Network*, edited by G.P. Crawford and S. Zumer (Taylor and Francis, London, 1995).
- [2] (a) D.W. Schaefer and K.D. Keefer, Phys. Rev. Lett. **56**, 2199 (1986); (b) D.W. Schaefer, Mat. Res. Soc. Bull. **19-4**, 49 (1994).
- [3] S. Faetti *et al.*, Phys. Rev. Lett. **55**, 1681 (1985).
- [4] T. Uchida and H. Seki, in *Liquid Crystals. Applications and Uses*, edited by B. Bahadur (World Scientific, Singapore, 1990), Vol. 3, Chap 5.
- [5] S. Kralj, G. Lahajnar, A. Zidan, M. Vilfan, R. Blinc, and M. Kosec, Phys. Rev. E **48**, 340 (1993).
- [6] A. Maritan, M. Cieplak, and J.R. Banavar, in Ref. [1].
- [7] P.A. Lebowitz and G. Lasher, Phys. Rev. A **6**, 426 (1972).
- [8] A. Maritan, M. Cieplak, T. Bellini, and J.R. Banavar, Phys. Rev. Lett. **72**, 4113 (1994).
- [9] T. Bellini *et al.*, Phys. Rev. Lett. **69**, 788 (1992); (b) T. Bellini and N.A. Clark in Ref. [1], Chap. 19; (c) T. Bellini, N.A. Clark, and D.W. Schaefer, Phys. Rev. Lett. **74**, 2740 (1995).
- [10] A.G. Rappaport, N.A. Clark, B.N. Thomas, and T. Bellini, in Ref. [1], Chap. 20.
- [11] G.S. Iannacchione, G.P. Crawford, S. Zumer, J.W. Doane, and D. Finotello, Phys. Rev. Lett. **71**, 2595 (1993); G.S. Iannacchione, G.P. Crawford, S. Qian, J.W. Doane, D. Finotello, and S. Zumer, Phys. Rev. E **53**, 2402 (1996).
- [12] L. Wu, B. Zhou, C.W. Garland, T. Bellini, and D.W. Schaefer, Phys. Rev. E **51**, 2157 (1995).
- [13] K. Uzelac, A. Hasmy, and R. Jullien, Phys. Rev. Lett. **74**, 422 (1995).
- [14] Z. Zhang and A. Chakrabarti (unpublished).
- [15] C. Zannoni, in *The Molecular Physics of Liquid Crystals*, edited by G.R. Luckhurst and G.W. Gray (Academic, London, 1979), Chap. 9.
- [16] U. Fabbri and C. Zannoni, Mol. Phys. **58**, 763 (1986).
- [17] Z. Zhang and O.G. Mouritsen, Phys. Rev. Lett. **69**, 203 (1992).
- [18] (a) C. Chiccoli, P. Pasini, F. Semeria, and C. Zannoni, Phys. Lett. A **150**, 311 (1990); (b) C. Chiccoli, P. Pasini, F. Semeria, and C. Zannoni, Mol. Cryst. Liq. Cryst. **212**, 197 (1992); (c) **221**, 19 (1992).
- [19] G.P. Crawford and J.W. Doane, Condens. Matter News **1**, 5 (1992).
- [20] C. Chiccoli, P. Pasini, F. Semeria, E. Berggren, and C. Zannoni, Mol. Cryst. Liq. Cryst. **266**, 241 (1995).
- [21] (a) E. Berggren, C. Zannoni, C. Chiccoli, P. Pasini, and F. Semeria, Chem. Phys. Lett. **197**, 224 (1992); (b) Phys. Rev. E **49**, 614 (1994); (c) **50**, 2929 (1994).
- [22] C. Chiccoli, P. Pasini, and C. Zannoni, Physica A **148**, 298 (1988).
- [23] T. Bellini, C. Chiccoli, P. Pasini, and C. Zannoni (unpublished).
- [24] A.J. Leadbetter, J.L.A. Durrant, and M. Rugman, Mol. Cryst. Liq. Cryst. **34**, 231 (1977).
- [25] G.R. Luckhurst and C. Zannoni, Nature (London) **267**, 412 (1977).